

Simulating Acoustic Propagation Using A Lattice Boltzmann Model Of Incompressible Fluid Flow

NATHAN FRASER[†] RICHARD HALL[§]

Dept. Computer Science & Engineering,
La Trobe University, Melbourne,
3086, Victoria, Australia

Abstract: Waveguide mesh models that simulate airborne acoustics require extra non-physical rules to accurately represent acoustic propagation collisions with objects. In this paper we describe a physics-based cellular automata of fluid flow phenomena which simulates acoustic as a by-product, in which such rules are unnecessary. We evaluate our simulation with respect to sound speed and boundary interactions. Applications include audio signal processing and computer generated sound.

Key- Words: Acoustics; Lattice Boltzmann;

1 Introduction

A digital waveguide mesh (DWM) is a finite-difference, time domain computational model that can simulate aspects of airborne acoustic (room) phenomena [1]. Spatial dimensions are discretised into a regular lattice of signal processing elements which are joined by unit delays and are updated synchronously in discrete time steps [2]. DWM have been applied to airborne, or room acoustics in 2-dimensions [1] and in 3-dimensions [3], with some limitations, which can be partly overcome by introducing additional rules at object boundaries [4]. Such rules appear to trade off the physical identity of DWM against computational expense (and perceived complexity) of physical models.

However, DWM are remarkably similar in design to lattice-based finite-difference physical models for fluid flow, whose origins lie in physical cellular automata models for self-reproduction [5], and lattice gas automata [6]. So-called lattice Boltzmann models (LBM) bear a remarkable resemblance to DWM except they calculate fluid mass interactions to solve the Navier-Stokes equations for fluid flow [7]. They have already been used to model acoustic wave generation in wind instruments [8], non-linear acoustics [9], and viscous acoustic absorption [10]. The possibility of using lattice Boltzmann models to simulate acoustic propagation has

been suggested [11].

In this paper, a LBM of incompressible fluid flow in 2-dimensions is tested for its ability to represent basic aspects of acoustic propagation. In [section 2](#) we outline the design of our model. We describe experiments which investigate the model's ability to represent sound speed and boundary interactions in [section 3](#). Finally, in [section 4](#) we outline future work and applications of the model.

2 Method

For empirical tests of the LBM, a 2-dimensional lattice with 9 fluid velocities (denoted D2Q9 in [Figure 1](#)) was used with a single relaxation time (ala [12]). The lattice structure is almost identical to that used for the interpolated rectilinear waveguide mesh [13]. We use a 2-dimensional lattice for two reasons: such approximations are able to represent many audio effects to acceptable accuracy [14]; and they can be warped to account for 3-D effects [15].

Lattice Boltzmann models compose a family of discrete-time discrete-velocity approximations of the Boltzmann equation for fluid flow:

$$\frac{\partial f}{\partial t} + \mathbf{v} \nabla f = \Omega(f)$$

Where statistical mass distributions f of particles move with velocity \mathbf{v} and are redistributed according to a kinetic collision function Ω [16]. Replacing

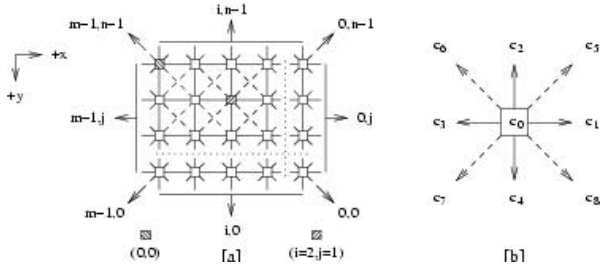


Figure 1: D2Q9 Topology: [a] Nodes are arranged in a 2-dimensional rectilinear lattice of size $m \times n$, with links to nearest (solid) and next-nearest (dashed) neighbours, and periodic boundaries as indicated. [b] Each fluid node has 9 link velocities $\mathbf{c}_0 \dots \mathbf{c}_8$ and three lattice speeds: 0, 1 and $\sqrt{2}$.

\mathbf{v} with a set of discrete velocities, and replacing the collision function Ω with a single relaxation time (τ) kinetic approximation [12] yields a discrete velocity Boltzmann equation [17]:

$$F_i(\mathbf{x} + \mathbf{c}_i \Delta t, t + \Delta t) - F_i(\mathbf{x}, t) = -\frac{1}{\tau} (F_i(\mathbf{x}, t) - F_i^{(eq)}(\mathbf{x}, t)) \quad (1)$$

Where the position of a node is denoted by \mathbf{x} , mass functions F_i represent the quantity of mass at that node moving according to the velocity \mathbf{c}_i and equilibrium functions $F_i^{(eq)}$ express the relax state of nodes, and hence the desired dynamics of the system. If $1/\tau$ is replaced with ω and Δt is set to 1, the state and evolution of nodes on the lattice with local mass density ρ , local momentum \mathbf{j} , and local velocity \mathbf{u} are described by:

$$\rho(\mathbf{x}, t) = \sum_i F_i(\mathbf{x}, t) \quad (2)$$

$$\mathbf{j}(\mathbf{x}, t) = \rho(\mathbf{x}, t) \mathbf{u}(\mathbf{x}, t) = \sum_i \mathbf{c}_i F_i(\mathbf{x}, t) \quad (3)$$

$$F_i(\mathbf{x} + \mathbf{c}_i, t + 1) = F_i + \omega (F_i^{(0)} - F_i) \quad (4)$$

The left hand side of (4) represents streaming of mass distributions to adjacent nodes along lattice velocities (see Figure 1), while the right hand side represents relaxation toward an equilibrium state that conserves local mass and momentum. The equilibrium functions $F_i^{(0)}$ chosen for the LBM tested in this paper are formed from a truncated power series of local momentum and mass density for the simulation of a linear and incompressible fluid flow:

$$F_i^{(0)}(\rho, \mathbf{j}) = \frac{W_i}{\rho_0} \left\{ \rho + \frac{1}{A} \mathbf{c}_i \cdot \mathbf{j} + \frac{1}{2\rho A} \left[\frac{1}{A} (\mathbf{c}_i \cdot \mathbf{j})^2 - \mathbf{j}^2 \right] \right\} \quad (5)$$

Weights W_i and the free parameter A are chosen to maximise stability of the underlying hydrodynamic system for all lattice sizes [18], and to obtain a solution at the macroscopic limit of the Navier-Stokes equations. The values used (as given in [7])

along with the discrete lattice velocities are:

$$\begin{aligned} \mathbf{c}_i &= (0, 0) & i &= 0 \\ \mathbf{c}_i &= (\pm 1, 0) & i &= 1, 3 \\ \mathbf{c}_i &= (0, \pm 1) & i &= 2, 4 \\ \mathbf{c}_i &= (\pm 1, \pm 1) & i &= 5, 6, 7, 8 \\ W_i/\rho_0 &= \frac{4}{9} & i &= 0 \\ W_i/\rho_0 &= \frac{1}{9} & i &= 1, 2, 3, 4 \\ W_i/\rho_0 &= \frac{1}{36} & i &= 5, 6, 7, 8 \\ A &= \frac{1}{3} \end{aligned} \quad (6)$$

Substituting these values into (5) gives the specific functions:

$$F_i^{(0)} = \begin{cases} \frac{4}{9} \rho \left[1 - \frac{1}{2} \mathbf{u}^2 \right] & i = 0 \\ \frac{1}{9} \rho \left[1 + 3 (\mathbf{c}_i \cdot \mathbf{u}) + \frac{9}{2} (\mathbf{c}_i \cdot \mathbf{u})^2 - \frac{1}{2} \mathbf{u}^2 \right] & i = 1, 2, 3, 4 \\ \frac{1}{36} \rho \left[1 + 3 (\mathbf{c}_i \cdot \mathbf{u}) + \frac{9}{2} (\mathbf{c}_i \cdot \mathbf{u})^2 - \frac{1}{2} \mathbf{u}^2 \right] & i = 5, 6, 7, 8 \end{cases} \quad (7)$$

Combining (2), (3), (4) and (7) produces a macroscopic Navier-Stokes approximation with a lattice sound speed of $c_s = 1/\sqrt{3}$. The acoustic pressure (p_a) and kinematic shear viscosity (ν) terms are [7]:

$$p_a(\mathbf{x}, t) \simeq (\rho(\mathbf{x}, t) - \rho_0) / 3 \quad (8)$$

$$\nu = \frac{2 - \omega}{6\omega} \quad (9)$$

Acoustic pressure is approximate since the application of input pressures by a small change in local mass density modifies average mass density, and the pressure is assumed to be proportional to density. ρ_0 is used as an approximation of the average which is correct only at initialisation. So long as input signals contain no DC offset, this approximation provides a valid estimate of acoustic pressure, as the average density on the lattice will remain close to ρ_0 .

Boundaries are considered in terms of inputs, outputs, and the intersection of free-space and objects. *Input* of pressure to the model is modeled by increasing the mass density at a chosen node by an amount proportional to the desired local pressure increase (p_{in}):

$$\Delta F_i(\mathbf{x}, t) = 3W_i p_{in} \quad (10)$$

Since pressure is distributed in a balanced fashion across the velocities, this does not introduce a net fluid velocity change for the input node. A pressure input may be applied to any free-space node on a lattice. *Outputs* involve measuring the acoustic pressure with (8), and since no change is made to the measured nodes, can be specified arbitrarily without affecting the model. *Solid obstacle* nodes

perform no relaxation step - each F_i is assigned a value from its opposite velocity:

$$\begin{aligned}
 F_0 &= F_0 \\
 F_{1,3} &= F_{3,1} \\
 F_{2,4} &= F_{4,2} \\
 F_{5,7} &= F_{7,5} \\
 F_{6,8} &= F_{8,6}
 \end{aligned}
 \tag{11}$$

This boundary is lossless and slightly error-prone, however it has better stability and is less computationally expensive than some other alternatives [19].

In our empirical experiments, a signal is input into a chosen lattice geometry and pressure measurements were taken at specific locations on the lattice for a chosen number of update steps. The values for p_a , mass distributions $F_{0\dots 8}$ and a temporary update array $F'_{1\dots 8}$ were stored in a multi-dimensional array. F_i 's were initialised from a specified ρ_0 then the steps [a-d] in Figure 2 were repeated. Output waveforms were analysed using the numerical computation package Octave [20] and visualisations were obtained from RMS pressure plot bitmaps, which were either normalised in amplitude or converted to a visual representation of relative sound pressure level in decibels (dB).

3 Results

For a model of acoustics to exhibit high physical correspondence, sound speed in the lattice must be close to actual sound speed, and interactions between propagating acoustic waves and object boundaries must be realistic. While the theoretical *sound speed* c_s for the D2Q9 model is supposedly

$1/\sqrt{3}$, in practice the sound wave travel speed is dependent both on frequency and ω . A coupling between velocity and viscosity [21] and model discretisation will affect the speed of acoustic propagation. To measure the effect of ω on average sound speed, a grid of size $l_x = l_y = 260$, $\rho_0 = 0.1$ was stimulated with an impulse of varying amplitudes ($a = 0.001, 0.01, 0.1, 0.2$) and run for 300 iterations. For each value of ω , impulse responses were obtained for positions in one octant at a distance of approximately 50 units from the input: $r \simeq 50$ and $0 < \theta < \pi/4$. Each measured point was analysed to determine the time to the first peak in the impulse response, and hence the propagation speed to that point. These speeds were then averaged and the results are graphed in Figure 3 along with the theoretical sound speed $1/\sqrt{3}$.

The measured sound speed was within 5% of c for values of ω over 1.1, and within 0.5% near 1.8. Increasing the amplitude of the impulse tended to slightly raise the sound speed travel, but only significantly when the input signal amplitude was similar or greater in magnitude than ρ_0 . No meaningful results were obtained for ω less than 0.5 since over-damping made the impulse response an inaccurate measure of sound speed.

We also demonstrate the acoustic propagation properties via pressure plots of D2Q9 with respect to three typical types of object boundaries: parallel reflection; diagonal reflection; and diffraction. Firstly, for *parallel reflection* Figure 4 shows a periodic plane wave incident on a solid wall, reflecting and setting up a standing wave pattern. The generated pattern shows incomplete cancellation at nodes because the discrete node lengths inexactly correspond with the wave travel speed $1/\sqrt{3}$ and wave period. Secondly, for *diagonal reflection*, Figure 5 shows a plane impulse wave incident on a wall at an angle of 45° . The plane wave reflects downward on the first impact [b], bounces between the wall angles [c], then returns, traveling to the left [d].

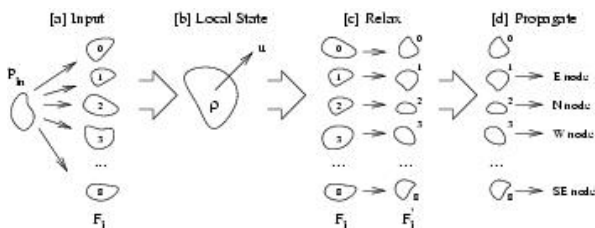


Figure 2: Node update process at each iteration: [a] Input pressure is converted to mass and distributed to the mass functions F_i . [b] Local mass density, velocity and pressure are calculated from the F_i . [c] Equilibrium functions $F_i^{(0)}$ and intermediate mass functions F'_i are computed. [d] F'_i are propagated to F_i at adjacent nodes along direction i (except rest mass F_0).

Finally, for *diffraction*, a simple slitted wall experiment is shown in Figure 6. A periodic plane wave is incident on a boundary with a slit of length 20. Pressure plots in normalised dB show the diffraction present at low frequencies, and the shadowing at higher ones.

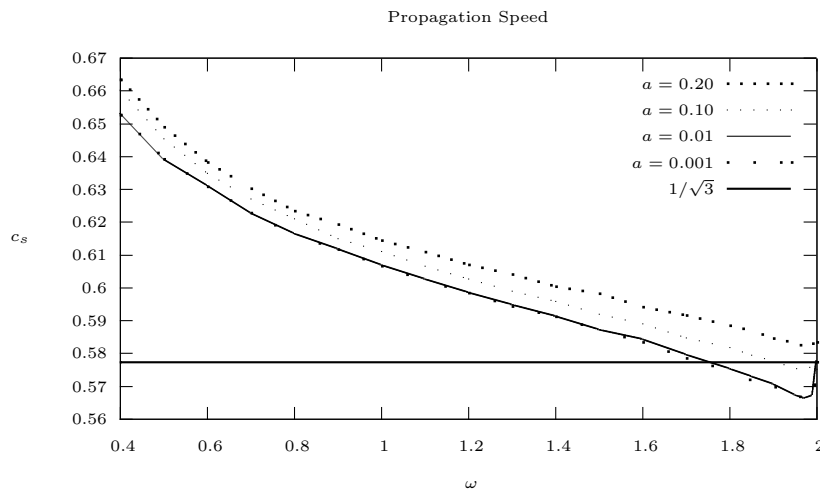


Figure 3: Measured sound propagation speed against ω over a range of impulse amplitudes. $\rho_0 = 0.1, r \simeq 50, 0 < \theta < \pi/4$

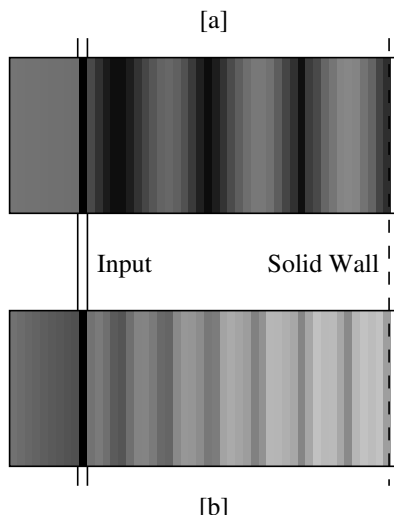


Figure 4: Generation of plane standing waves by a plane wave incident on a solid wall ($\omega = 1.8, l_x = 800$). [a]: $f = 0.025$ [b]: $f = 0.05$.

4 Conclusion

In this paper we described the use of a physical cellular automata model for computational fluid dynamics which was subverted to simulate acoustic propagation in a fluid medium. We demonstrated that our model D2Q9 represents sound speed and object boundary interactions reasonably realistically without the need for additional boundary rules (ala DWM), thus it has good physical correspondence. Operation of the model is independent of lattice geometry and the relative positions

of sources and sinks, allowing accurate simulation even if this geometry changes during simulation.

The fluid-based approach to simulating acoustics is also being evaluated in terms of scalability and operational frequency range. With *scalability*, we wish to exploit the regular structure and communication patterns of Lattice Boltzmann models in order to achieve real-time simulation of room acoustics with arbitrary geometry. With *operational frequency range*, we want to know if the model has the same limits of digital waveguide meshes, and if the alternative approach can improve on current interpolation and digital filtering techniques. Boundary condition geometry is easily specified in lattice-based models but, while simple boundaries are trivially implemented, they are typically non-physical and cannot represent an absorptive boundary accurately. Many boundary methods are available from LBM research and we intend to evaluate these in comparison with DWM boundaries for simulations of room acoustics with lossy boundaries.

There exist several potential applications of the model, such as physically correct simulation, imaginary musical instrument sound synthesis, and educational purposes. The first application is desired in digital signal processing, audio engineering, sound synthesis and music. The second application can be achieved using small lattice sizes that can be computed in real-time that simulate a musical instrument with arbitrary, perhaps impossible, geometry, whose output is still based on

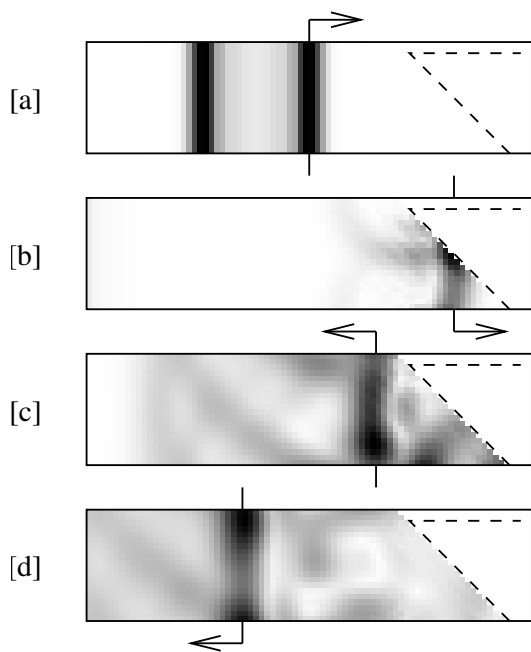


Figure 5: Four stages from a simulation of a plane wave obliquely reflecting on a diagonal boundary and then returning in the opposite direction. [a]: $t = 15$ [b]: $t = 60$ [c]: $t = 120$ [d]: $t = 160$

physical behaviour. These instruments could be controlled using a graphical interface or optimised from a desired output profile. Such a graphical interface could also allow the model to be used for educational purposes. Acoustic wave propagation could be presented at several time scales with various types of signals. Furthermore, since an understanding of the update process at each node can be reached without an understanding of mathematical methods, the model could be used as an introduction to computational and numerical methods for solving difficult equations.

References

[1] Mullen J., Howard D.M., and Murphy D.T. Digital Waveguide Modelling of the Vocal Tract Acoustics. In *Proceedings of the IEEE Workshop on Applications of Signal Processing to Audio and Acoustics*. New Paltz, NY, Oct. 2003.

[2] van Duyne S.A. and Smith III J.O. Physical modeling with the 2-D digital waveguide mesh. In *Proceedings of the International Computer Music Conference*. Tokyo, Japan, sep 1993.

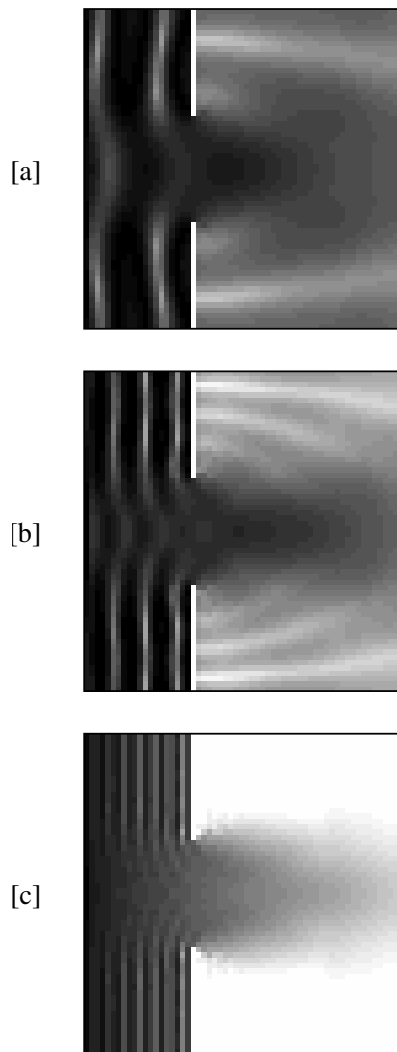


Figure 6: Wave propagation through a slit of length = 20. Pressure fields are displayed in dB, white is $\le -60\text{dB}$. [a]: $f = 0.025$ [b]: $f = 0.05$ [c]: $f = 0.1$.

[3] Savioja L. and Lokki T. Digital waveguide mesh for room acoustic modeling. In *ACM Siggraph Campfire: Acoustic Rendering for Virtual Environments*. Snowbird, Utah, May 2001.

[4] Laird J., Masri P., and Canagarajah N. Modelling Diffusion at the Boundary of a Digital Waveguide Mesh. In *Proceedings of the International Computer Music Conference*. Beijing, China, Oct. 1999.

[5] von Neumann J. *Theory of self-reproducing automata*. University of Illinois Press, 1966. Edited and completed by Arthur W. Burks.

[6] Toffoli T. and Margolas N. *Cellular Automata Machines*. MIT Press, Cambridge, MA, 1987.

- [7] Wolf-Gladrow D.A. *Lattice-Gas Cellular Automata and Lattice Boltzmann Models, An Introduction*, vol. 1725 of *Lecture Notes in Mathematics*. Springer-Verlag, Berlin, 2000.
- [8] Kühnelt H. Simulating the mechanism of sound generation in flutes using the lattice boltzmann method. In *Proceedings of the Stockholm Music Acoustics Conference*. Stockholm, Sweden, Aug. 2003.
- [9] Buick J.M., Greated C.A., and Gilbert J. Lattice Boltzmann BGK simulation of nonlinear sound waves: the development of a shock front. *Journal of Physics A*, vol. 33, 2000, pp. 3917–3928.
- [10] Fraser N. and Hall R. Extending the waveguide mesh to represent viscous absorption. *WSEAS Transactions on Acoustics and Music*, vol. 1(2), 2005, pp. 5–10.
- [11] Buick J.M., Neal M.A., and Campbell D.M. The Lattice Boltzmann Model and its Application to Acoustics. In *Proceedings of the 17th International Congress on Acoustics*. Rome, Italy, 2001.
- [12] Bhatnagar P.L., Gross E.P., and Krook M. A model for collision processes in gases. I. Small amplitude processes in charged and neutral one-component systems. *Physical Review*, vol. 94(3), May 1954, pp. 511–525.
- [13] Savioja L. and Välimäki V. Improved discrete-time modeling of multi-dimensional wave propagation using the interpolated digital waveguide mesh. In *Proceedings of IEEE International Conference on Acoustics, Speech, and Signal Processing ICASSP-97*, vol. 1, Apr. 1997.
- [14] Murphy D.T. and Howard D.M. 2-D Digital Waveguide Mesh Topologies in Room Acoustic Modelling. In *Proceedings of the COST G-6 Conference on Digital Audio Effects*. Verona, Italy, Dec. 2000.
- [15] Chopard B., Luthi P.O., and Wagen J.F. Lattice Boltzmann method for wave propagation in urban microcells. *IEE Proceedings—Microwaves, Antennas and Propagation*, vol. 144(4), Aug. 1997, pp. 251–255.
- [16] Buick J.M. Lattice Boltzmann Methods in Interfacial Wave Modelling. Ph.D. thesis, University of Edinburgh, 1997. <http://www.ph.ed.ac.uk/~jmb/thesis/tot.html>.
- [17] Sterling J.D. and Chen S. Stability Analysis of lattice Boltzmann Methods. *Journal of Computational Physics*, vol. 123, 1996, pp. 196–206.
- [18] Worthing R.A., Mozer J., and Seeley G. Stability of lattice Boltzmann methods in hydrodynamic regimes. *Physical Review E*, vol. 56(2), 1997, pp. 2243–2253.
- [19] Zou Q. and He X. On pressure and velocity flow boundary conditions and bounceback for the lattice Boltzmann BGK model. *Physics of Fluids*, vol. 9, 1997, pp. 1591–1598.
- [20] Eaton J.W. GNU Octave, a high-level language, primarily intended for numerical computations. <http://www.octave.org/>.
- [21] Qian Y.H. and Zhou Y. Complete Galilean-Invariant Lattice BGK Models for the Navier–Stokes Equation. *Europhysics Letters*, vol. 42(4), 1998, pp. 359–364.